Base Stacking in Adenosine Dimers Revealed by Femtosecond Transient Absorption Spectroscopy

ARTICLE *in* JOURNAL OF THE AMERICAN CHEMICAL SOCIETY · APRIL 2014

Impact Factor: 12.11 · DOI: 10.1021/ja501342b · Source: PubMed

2 AUTHORS:

Jinquan Chen
East China Normal University
12 PUBLICATIONS **100** CITATIONS
SEE PROFILE

Bern Kohler
Montana State University
109 PUBLICATIONS **4,770** CITATIONS
SEE PROFILE

JACS
JOURNAL OF THE AMERICAN CHEMICAL SOCIETY

Article

pubs.acs.org/JACS

Base Stacking in Adenosine Dimers Revealed by Femtosecond Transient Absorption Spectroscopy

Jinquan Chen and Bern Kohler*

Department of Chemistry and Biochemistry, Montana State University, Bozeman, Montana 59717-3400, United States

Supporting Information

ABSTRACT: Excitons formed in DNA by UV absorption decay via poorly understood pathways that can culminate in mutagenic photoproducts. In order to gain insight into how base stacking influences UV excited states in DNA, five dinucleosides composed of adenosine or 2′-deoxyadenosine units joined by flexible linkers were studied by femtosecond transient absorption spectroscopy. In aqueous solution, transient absorption signals recorded at pump and probe wavelengths of 267 and 250 nm, respectively, show that UV absorption produces excimer states in all dimers that decay orders of magnitude more slowly than excitations in a single adenine nucleotide. Adding methanol as a cosolvent disrupts $\pi-\pi$ stacking of the adenine moieties and causes the excimer states in all five dinucleosides to vanish for a methanol concentration of 80% by volume. These observations confirm that base stacking is an essential requirement for the slow decay channel seen in these and other DNA model compounds. This channel appears to be insensitive to the precise stacking conformation at the instant of photon absorption as long as the bases are cofacially stacked. Notably, circular dichroism (CD) spectra of several of the dinucleosides are weak and monomer-like and lack the exciton coupling that has been emphasized in the past as an indicator of base-stacked structure. For these dimers, the coupled transition dipole moments of the two adenines are proposed to adopt left- and right-handed arrangements upon stacking with roughly equal probability. Although the mechanism behind slow nonradiative decay in DNA is still uncertain, these results show that the signature of these states in transient absorption experiments can be a more reliable diagnostic of base stacking than the occurrence of exciton-coupled CD signals. These observations also draw attention to the important role the backbone plays in producing structures with axial (helical) chirality.

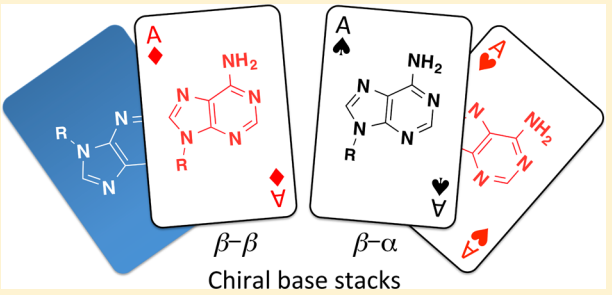

INTRODUCTION

During the past decade, there have been many advances in understanding the nature and dynamics of excited electronic states in nucleic acids.[1−5] Mounting evidence indicates that $\pi-\pi$ stacking between adjacent bases profoundly affects excited-state relaxation and is responsible for long-lived excited states that are readily detected in transient absorption (TA) experiments.[6−8] The acute sensitivity of excited-state dynamics to $\pi-\pi$ interactions between bases illuminates an opportunity to use femtosecond TA spectroscopy to study conformational dynamics of nucleic acids. Unlike existing structural probes such as NMR and circular dichroism (CD), femtosecond pump−probe measurements are capable in principle of responding to and reporting on structural dynamics that take place on subnanosecond time scales. In order to realize this promise, a full understanding of how structure and structural dynamics affect DNA excited states is required.

In this work, we report on the sensitivity of TA measurements to $\pi-\pi$ stacking interactions by the two bases in a series of dinucleosides, which serve as simple models of single DNA and RNA strands. Structural dynamics of single-stranded nucleic acids influence many fundamental events in molecular biology including RNA folding,[9] protein−DNA binding,[10,11] DNA melting,[12] telomere dynamics,[13] and DNA photodamage.[14−16] Unfortunately, single-stranded nucleic acids are rarely amenable to study by X-ray diffraction due to their conformational lability, and there is considerable uncertainty about their static and dynamic structural properties. Molecular dynamics (MD) simulation is one of the only general techniques that provides information with both high spatial and temporal resolution, but the dynamical predictions from these theoretical calculations are largely unchecked by experiment. Growing evidence[17] that MD force fields overstabilize base stacking interactions makes the need for experimental probes of single strand structure and dynamics especially important.

Here, we employ deep UV femtosecond TA spectroscopy to investigate the dynamics of excited electronic states formed by UV excitation of the five diadenosine compounds shown in Chart 1. Dimers of (2′-deoxy)adenosine were chosen because of the high propensity of adenine to associate by cofacial stacking in aqueous solution. Vapor pressure osmometry experiments,[18] CD,[19−23] UV hypochromism,[22,24−26] calorim-

Received: February 8, 2014

   dx.doi.org/10.1021/ja501342b | J. Am. Chem. Soc. XXXX, XXX, XXX−XXX

Chart 1. Structures and Abbreviations of the Dinucleosides Studied

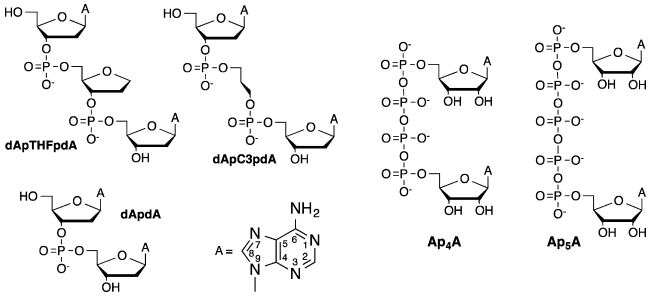

etry,[27−29] and single-molecule stretching experiments[30,31] all provide evidence for the high stacking ability of adenine.[32] Calculations also predict that purine-on-purine stacking is most favored in aqueous solution.[33] The three diadenosine compounds on the left side of Chart 1 have 2′-deoxyribose sugars connected via the normal 3′-5′ linkages found in natural nucleic acids. The diadenosine monophosphate 2′-deoxyadenylyl (3′-5′) 2′-deoxyadenosine (dApdA) is the smallest subunit of natural DNA that exhibits adenine-on-adenine base stacking. In dApTHFpdA, a tetrahydrofuran derivative mimics an abasic site in the closed hemiacetal geometry. The flexible three-carbon (propyl) linker in dApC3pdA is a further model of an abasic site. Finally, the long linkers and multiply charged phosphate groups in the 5′,5′-linked diadenosine oligophosphates P^1,P^4-di(adenosine-5′)tetraphosphate (Ap_4A, Chart 1) and P^1,P^5-di(adenosine-5′)pentaphosphate (Ap_5A, Chart 1) were chosen because prior work suggests that these compounds stack quite differently than the DNA forms.[34,35] This study reveals that the excimer states seen in TA experiments on nucleobase dimers are only observed in π-stacked conformations, but the lifetimes of these states are insensitive to how the stacked bases are oriented. It is further shown that CD spectra can sometimes lead to unreliable conclusions about base stacking, but the detection of excimer states in TA experiments is a robust predictor of this interaction.

RESULTS

Steady-State Spectroscopy. UV−vis absorption spectra of all five diadenosines and their monomer model compounds are very similar as shown and discussed in Figures S1 and S2. In contrast, pronounced differences are seen in the room-temperature CD spectra in aqueous solution (Figure 1) and in 80% methanol (Figure 2). [The percentage of methanol by volume will be used to designate all methanol−water solutions, e.g., 80% methanol designates a solvent that is 80% methanol and 20% water (v/v).] The CD spectrum of dApdA (Figure 1a, blue curve) matches previously reported spectra in shape,[36,37] and $\Delta\varepsilon$ values at extremal points agree within 10% with previous measurements.[23,38] The dApdA CD spectrum shows a positive Cotton effect with a maximum near 270 nm, followed by a negative Cotton effect of approximately equal peak area with a minimum at 250 nm. This bisignate signal arises from degenerate exciton coupling and will be referred to henceforth as a (positive) couplet. The zero crossing at 261 nm occurs at the approximate location of the band maximum seen in the UV−vis absorption spectrum.[39] A second, more intense positive couplet occurs for dApdA between 200 and 230 nm (Figure 1a).

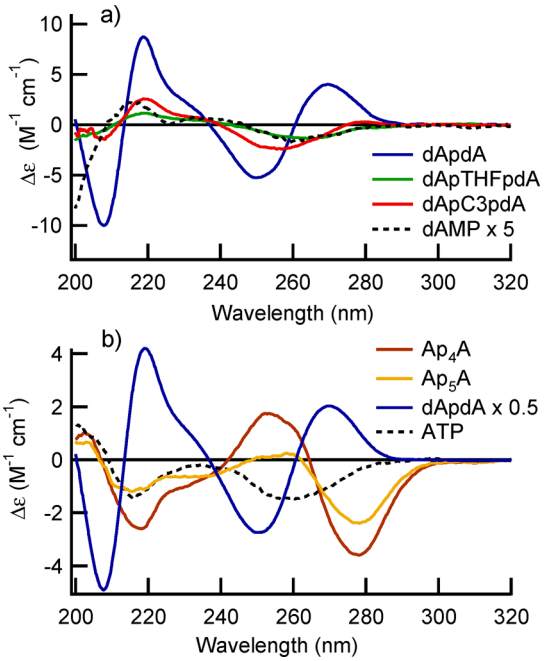

Figure 1. CD spectra in aqueous buffer solution: (a) dApdA, dApTHFpdA, dApC3pdA, and dAMP (× 5); (b) Ap_4A, Ap_5A, dApdA (× 0.5), and ATP. Spectra from compounds with one vs two adenosines are shown by dashed and solid curves, respectively.

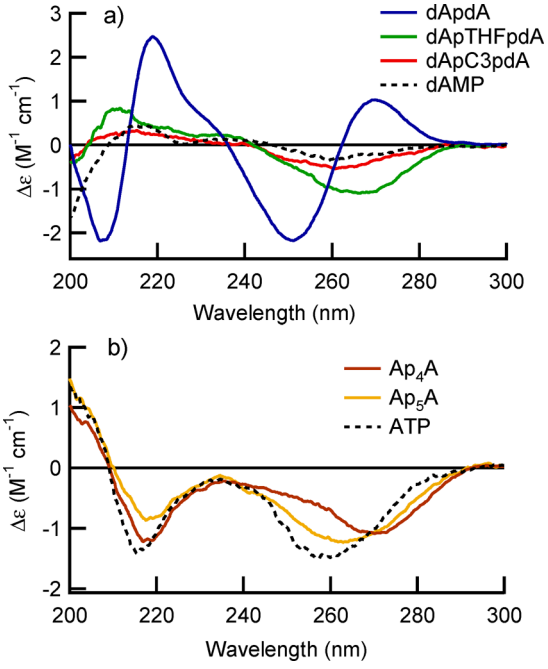

Figure 2. CD spectra in 80% methanol/20% water (v/v) solution at room temperature: (a) dApdA, dApTHFpdA, dApC3pdA, and dAMP; (b) Ap_4A, Ap_5A, and ATP.

CD spectra of dApTHFpdA and dApC3pdA (Figure 1a) have not been reported previously. The signals are several times less intense than the CD spectrum of dApdA, and a positive couplet is absent at long wavelengths. Instead, dApTHFpdA and dApC3pdA show minimum CD signals at 265 and 255 nm, respectively. The CD spectrum of dApC3pdA shows a very weak positive band with a maximum near 280 nm and a zero crossing at 275 nm compared to 261 nm for dApdA. Overall,

dx.doi.org/10.1021/ja501342b | J. Am. Chem. Soc. XXXX, XXX, XXX−XXX

the spectra of both dimers resemble that of the monomer 2′-deoxyadenosine 5′-monophosphate (dAMP) but have greater amplitude. The weak CD spectrum of dAMP agrees with the literature.[40]

CD spectra of the two oligophosphates Ap_4A and Ap_5A are compared with the CD spectra of dApdA and adenosine 5′-triphosphate (ATP) in Figure 1b. A broad negative peak with a minimum near 260 nm is seen for ATP in good agreement with the spectrum for this compound reported by Heyn and Bretz at low concentration and in 1 M Tris-HCl buffer, 0.5 M $MgCl_2$ at pH 8.7.[41] Strikingly, bands in the CD spectra of Ap_4A and Ap_5A in aqueous solution are opposite in sign compared to those in the dApdA CD spectrum (Figure 1b) as first reported by Zamecnik and co-workers.[34,42] The CD spectrum of Ap_4A has a negative peak with $\Delta\varepsilon = -3.0\ M^{-1}\ cm^{-1}$ at 278 nm and a positive peak with $\Delta\varepsilon = +1.4\ M^{-1}\ cm^{-1}$ at 250 nm. The CD spectrum of Ap_5A has a negative peak with $\Delta\varepsilon = -2.0\ M^{-1}\ cm^{-1}$ at 278 nm and a positive peak with $\Delta\varepsilon = +0.2\ M^{-1}\ cm^{-1}$ at 260 nm. These values agree reasonably well with ones reported by Holler et al.[42] in Tris-HCl buffer at pH 7.5 after dividing their signals by two to give per residue quantities. The ratio of the amplitude of the positive peak at 252 nm to the negative peak at 278 nm (i.e., peak-to trough ratio[42]) is 0.5 in our spectrum compared to 0.6 in the spectrum recorded by Holler et al.[42] This difference could be due to the different pH buffer used here or the nature of the counterions (lithium in ref 42, sodium in this work).

The CD spectra of the five dinucleosides and the monomers ATP and dAMP in 80% methanol are shown in Figure 2. CD spectra of dApTHFpdA and dApC3pdA are weak and closely resemble that of dAMP (Figure 2a). The oligophosphates Ap_4A and Ap_5A also have weak CD spectra that are similar to the CD spectrum of ATP (Figure 2b). Comparison with Figure 1 reveals that the CD spectra of dAMP and ATP in 80% methanol are very similar to the spectra recorded in buffer solution. dApdA is the only one of the five dimers that exhibits a CD spectrum in 80% methanol that differs substantially from its corresponding monomer model compound. This spectrum, which is approximately three times weaker than in buffer solution, still features a positive couplet between 240 and 290 nm that resembles the one seen in aqueous solution. In addition, the zero crossing point seen near 261 nm in water moves to 263 nm in 80% methanol. The CD spectrum of dApdA in water at pH 2 also deviates from the monomer CD spectrum and has a bisignate appearance above 240 nm (Figure 3).

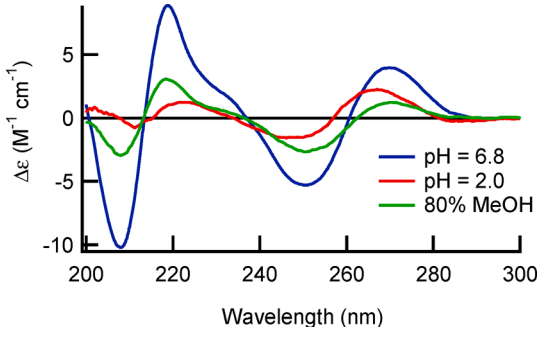

Figure 3. CD spectra of dApdA at pH = 6.8 (blue curve) and pH = 2.0 (red curve) and in 80% methanol/20% water (v/v) solution (green curve).

TA Kinetics in Aqueous Solution at Room Temperature. Pump−probe signals recorded in aqueous buffer solution at a pump wavelength of 266 nm and a probe wavelength of 250 nm (hereafter: 266/250 nm) for the three dimers of 2′-deoxyadenosine, dApdA, dApTHFpdA, and dApC3pdA, show a strong bleach immediately after time zero (Figure 4). TA signals in this and later figures have been

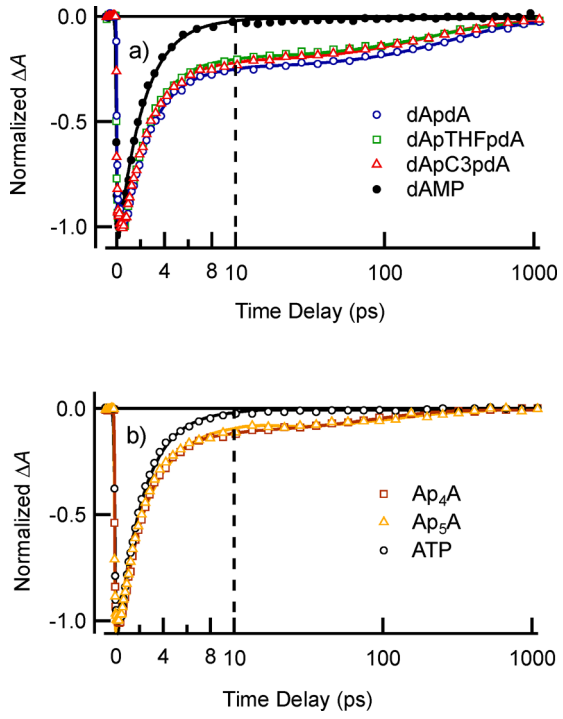

Figure 4. TA signals (266 nm pump/250 nm probe) in aqueous buffer solution: (a) dAMP, dApdA, dApTHFpdA, and dApC3pdA; (b) ATP, Ap_4A, and Ap_5A.

normalized to have the same maximum bleach amplitude. The absolute signals depend on the pump pulse fluence, but in a typical measurement the absorbance change seen near time zero for dApdA is approximately −0.003.

The dimer signals exhibit an obvious long-lived component not seen in the pump−probe signal of the mononucleotide dAMP. Normalized TA signals (266/250 nm) for the diadenosine oligophosphates Ap_4A and Ap_5A exhibit long-lived decay components in aqueous buffer solution (Figure 4b), which resemble the ones seen in the 2′-deoxyadenosine dimers (Figure 4a). The bleach signals for Ap_4A and Ap_5A in buffer solution agree within experimental uncertainty. The triphosphate monomer ATP shows no long-lived decay component under the same conditions (Figure 4b). In fact, 266/250 nm pump−probe signals for ATP and dAMP are indistinguishable within experimental uncertainty (Figure S3), indicating that the excited-state dynamics of a single adenine residue are independent of the number of phosphate groups and the presence or absence of the 2′-OH group of ribose. For the monomers, the bleach signals recover with a single time constant of 2.2 ± 0.2 ps in good agreement with the value of 2.01 ± 0.09 ps reported by Su et al.[8]

The TA signals in Figure 4 were fit to a sum of three exponentials plus an offset. A subpicosecond component (τ_1) with positive amplitude causes the initial bleach amplitude to increase slightly in magnitude during the first ps after excitation

dx.doi.org/10.1021/ja501342b | J. Am. Chem. Soc. XXXX, XXX, XXX−XXX

as seen in the short-time scale dynamics in Figure S4. This signal component is not seen in the TA signals of any of the adenine monomers. Time constants were mostly globally linked, but slightly better fits as judged by the minimum AICc value (see description of the fitting procedure in Supporting Information) were obtained by separately linking τ_3 for the 2′-deoxyadenosine dimers (Table S1). As shown in the table, common lifetimes of 0.32 ± 0.13, 2.20 ± 0.13, 110 ± 20 (diadenosine oligophosphates), and 210 ± 30 ps (2′-deoxyadenosine dimers) were obtained.

The lifetime of 210 ± 30 ps determined for the 2′-deoxyadenosine dimers agrees well with the value of 183 ± 6 ps reported recently by Su et al. for a set of variable-length $(dA)_n$ oligonucleotides that included the dimer dApdA.[8] The lifetime of 110 ± 20 ps observed for Ap_4A and Ap_5A is similar to the value of 105 ± 30 ps reported for the RNA dinucleoside monophosphate ApA.[7] The possibility of distinct lifetimes for A-A stacks having ribose vs 2′-deoxyribose sugars is intriguing, but more work is needed to confirm this possibility. We note that a global fit with the same τ_3 value for all five dinucleoside TA signals in Figure 4 produces an AICc value that is only slightly larger than the fit in Table S1.

TA Kinetics in Methanol–Water Solutions at Room Temperature. Increasing the concentration of methanol in a methanol–water solvent mixture progressively attenuates the long-lived signal component observed in TA signals from dApdA and dApTHFpdA (Figure 5). These signals were fit to

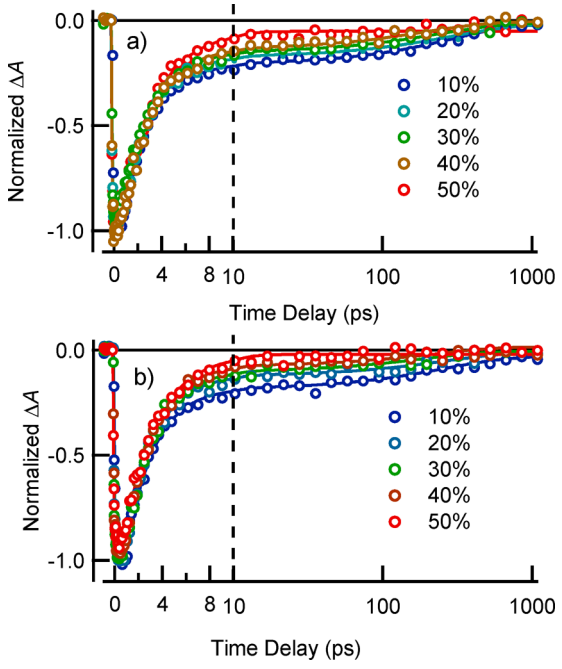

Figure 5. TA signals (266 nm pump/250 nm probe) from (a) dApdA and (b) dApTHFpdA in methanol–water solutions as a function of the percent methanol by volume.

three exponentials plus a constant offset (Table S2). As the percentage methanol is increased, the amplitude of the τ_3 component (A_3 in Table S2) decreases until the long-lived component is no longer detectable for methanol concentrations above about 50%. Notably, the subpicosecond decay component (τ_1) appears unchanged as the fraction of methanol is increased.

The long-lived component (τ_3) observed for all five diadenosine dimers in aqueous solution vanishes in 80% methanol solution (Figure 6). The signals were fit to two

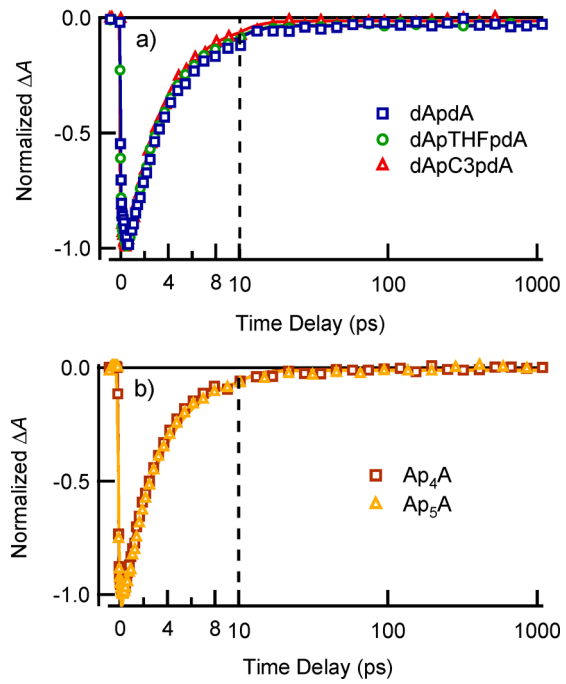

Figure 6. TA signals (266 nm pump/250 nm probe) in 80% methanol/20% water (v/v) solution: (a) dApdA, dApTHFpdA, and dApC3pdA; (b) Ap_4A, and Ap_5A.

exponentials plus an offset (Table S3). The subpicosecond component (τ_1 = 0.31 ± 0.12 ps) has the same value within experimental uncertainty in 80% methanol as in buffer solution. The second lifetime, τ_2, has values of 3.20 ± 0.12 and 2.92 ± 0.11 ps for the 2′-deoxyadenosine and adenosine dimers, respectively. These lifetimes are about 40% larger than the τ_2 values observed for the five dimers in buffer solution.

DISCUSSION

In this study, CD and TA signals were recorded for the five diadenosines in Chart 1 in aqueous and in methanolic solution. The different backbones and solvent conditions perturb both the extent of π–π stacking between the adenines in these compounds and the geometries of the stacked conformations. Detailed comparison of the CD and TA signals, which is undertaken here for the first time, clarifies the sensitivity of each technique to base stacking in dinucleotides. A striking observation is the similar dynamics seen for the TA bleach signals of the various adenine dimers in aqueous solution. In every case, a long-lived decay component of ~200 ps is observed, which was previously assigned to excimer states.[6,8,43] In the presence of a destacking cosolvent (methanol), this component vanishes. As discussed below in more detail, this is strong evidence that π–π stacking between the bases of each of the five adenosine dimers is required for excimer formation.

In contrast to the similar TA bleach kinetics, the CD spectra of the five compounds are remarkably diverse. The following discussion focuses on reconciling the different and occasionally contradictory observations from CD and TA spectroscopy. It will be shown that the long-lived decay component in the TA signals is only observed when the adenines are intimately π-

dx.doi.org/10.1021/ja501342b | J. Am. Chem. Soc. XXXX, XXX, XXX–XXX

stacked with one another, yet the lifetime of this decay is insensitive to the stacking geometry. On the other hand, exciton-coupled CD (ECCD) spectra, which are often observed when two or more nucleobases are $\pi-\pi$ stacked, will be shown to sometimes be an unreliable indicator of base stacking. The remainder of this section is organized as follows: First, the evidence that only stacked bases yield excimer states will be presented, followed by a discussion of how the signs and strengths of the couplets measured in ECCD spectra can be predicted from the orientation of two adenines in a cofacial stack. Using modern values of the transition dipole moment directions of adenine, it will then be argued that the five diadenosines studied here stack in quite different ways, yet have very similar excimer lifetimes. Finally, the implications of these findings for excimer states in DNA and for diagnosing base stacking by CD spectroscopy will be discussed.

Excimers Are Observed for All Diadenosines in Aqueous Solution. TA signals recorded at a probe wavelength of 250 nm (Figures 4−6) are negative ($\Delta A < 0$) for all of the diadenosines studied, indicating that the 250 nm probe pulse is absorbed more strongly by ground state molecules than by transient states created by the pump pulse. The decay of these ground-state bleaching (GSB) signals measures the time needed to repopulate the electronic ground state. Following an initial growth in the GSB signal with a time constant of approximately 300 fs (τ_1), the signals in aqueous solution recover biexponentially toward $\Delta A = 0$ with a time constant of a few picoseconds (τ_2) and a slow component of between 100 and 200 ps (τ_3). A weak offset of 1 or 2% seen in all TA signals may be due to photodegradation resulting from photoionization or some other process and will not be considered further due to its negligible amplitude. Fitting parameters for all transients are summarized in Tables S1−S3.

The τ_1 and τ_2 components are assigned to monomer-like dynamics due to ultrafast internal conversion and vibrational cooling in both aqueous and methanolic solution. When an excited base monomer decays by internal conversion to the electronic ground state on a subpicosecond time scale, GSB signals recorded at UV probe wavelengths recover predominantly at a rate that reflects intermolecular energy transfer to the solvent.[3,44] The τ_2 decay is thus assigned to vibrational cooling after ultrafast internal conversion.[3] This assignment is supported by the slower τ_2 decay seen in methanol compared to aqueous solution. The τ_2 lifetime of ∼3 ps (Table S3) observed in 80% methanol for all diadenosines is 40% longer than the 2.2 ps lifetime measured in water (Table S1). Earlier, vibrational cooling by 9-methyladenine in neat methanol was monitored at the same probe wavelength and shown to occur with a time constant of 4.5 ± 0.6 ps compared to 2.4 ± 0.4 ps in water.[45] The shorter vibrational cooling time observed here for dApdA in 80% methanol vs 9-methyladenine in 100% methanol is reasonable because the small amount of water in the former solvent should accelerate intermolecular energy transfer.[44] The longer value of τ_2 in 80% methanol is consistent with monomer-like ultrafast internal conversion in nucleobases that are unstacked and surrounded by solvent molecules. The identity of the τ_1 decay is less certain[45] but may reflect the time required for the excited-state population to reach the hot ground state.

The τ_3 component arises from long-lived (LL) excited states, which have been detected in previous TA experiments carried out on a variety of single- and double-stranded DNAs.[3,4] Although most excited states of single DNA bases decay to the ground state within several hundred femtoseconds, excited states of DNA oligomers and polymers commonly decay orders of magnitude more slowly. The long-lived excited states arise from interactions between the two adenine residues as seen by the absence of a long-lived decay component in the monomers AMP and ATP (Figure 4). Although there has been some disagreement about the nature of the long-lived excited states seen in base-stacked DNA, we refer to these states hereafter as excimers in agreement with discussion elsewhere.[3,43,46−53] In addition to their contribution to the TA signals, excimers are responsible for much of the subnanosecond emission seen from oligonucleotides.[49,53]

Excimers Are Not Observed When the Bases Are Unstacked. Excimers are not seen for any of the diadenosines in 80% methanol (Figure 6), and the TA signals instead agree with those of the monomers AMP and ATP. Organic solvents such as methanol denature double-stranded DNA[54,55] and disrupt base stacking in single-stranded DNA and RNA.[21] For example, adding ethylene glycol to the diribonucleoside monophosphate ApA mimics the effect of increasing the solution temperature.[56] Earlier, Cantor et al.[57] showed that the CD spectra of linear and cyclic deoxythmidine dimers become monomer-like in methanol solution and lack exciton-coupled features. High methanol concentrations are believed to produce unstacked states in which the two bases have no contact between their π faces and are separated by one or more solvent molecules. The absence of long-lived excited states in 80% methanol strongly supports the conclusion that excimer formation only occurs when the adenine residues are $\pi-\pi$ stacked at the instant of excitation. ECCD features can still be observed for dApdA in methanol (see below), but excimer formation is eliminated. This indicates that excimer formation results from a shorter-range interaction than the one responsible for the ECCD spectrum. We propose that the orbital−orbital overlap that arises in π-stacked conformations is a requirement for excimer formation by two nucleobases.

The observation of excimer signals in all five diadenosines in aqueous solution (Figure 4) indicates that the various linkers do not hinder these compounds from folding into base-stacked conformations. The count of single bonds linking the N9 atoms of the two residues by the shortest path is 11, 17, 17, 18, and 20 for dApdA, dApC3pdA, dApTHFpdA, Ap_4A, and Ap_5A, respectively. The longer linkers must be sufficiently flexible to permit the hydrophobic bases to stack. Earlier, Kool and coworkers demonstrated that emission from an α-pyrene deoxyriboside excited at 340 nm is strongly quenched by an adjacent thymine when these two moieties are separated by the standard phosphodiester linker or a C3 spacer.[58] Because emission quenching is thought to involve electron transfer from pyrene to thymine,[58] and because electron transfer is strongly gated by base stacking,[59−61] these results support our finding that a C3 spacer does not impede $\pi-\pi$ stacking between the flanking nucleobases.

ECCD Spectra Constrain the Possible Geometries of Stacked Bases. Excimer formation is clearly gated by base stacking, but how does the geometry of the stack affect excimer formation and decay? Although the stacking geometry between two bases in a single strand of duplex DNA can be a starting point for thinking about the stacking preferences of dinucleotides, the evidence discussed below strongly suggests that the diadenosines studied here adopt quite different geometries. This section discusses how conclusions about geometry are obtained from CD spectra. CD spectroscopy is

dx.doi.org/10.1021/ja501342b | J. Am. Chem. Soc. XXXX, XXX, XXX−XXX

exquisitely sensitive to the mutual orientation of chromophores through the pattern of Cotton effects that are observed as a function of wavelength. The pronounced variation in the CD spectra of the five diadenosines in aqueous solution (Figure 1) thus indicates that they form stacks with different geometries. Here, we will only consider cofacial stacks in which the two bases are restricted to lie in parallel planes. Even with this restriction, the stacked geometry depends on the twist angle (defined below), on the displacement of one of the two bases in a direction parallel to the base planes, and on which of two distinguishable sides of each base (front and back, see below) are in van der Waals contact.

The distinctive bisignate CD signals seen for several of the diadenosines arise from exciton coupling, which results from electrostatic interactions among transition dipole moments located on nearby bases.[39,62] We assume in the following that the mutual orientation of the stacked nucleobases makes the greatest contribution to the ECCD spectrum, and we ignore conformational details of the sugar groups and linker, which make only minor contributions to the ECCD signals. In this limit, ECCD is a consequence of how the achiral nucleobases are arranged around a chirality axis oriented perpendicular to the base planes, which are assumed to be parallel to one another.

For degenerate coupling—the coupling that dominates the ECCD spectra of homodimers like the ones in this study—transition dipoles corresponding to the same electronic transition on different bases interact with one another. The ECCD signal strength, $\Delta\varepsilon$, is proportional to the product of the interaction energy or Coulombic coupling between the two transition dipoles, V_{12}, and a scalar triple product:[63]

$$\Delta\varepsilon \propto \vec{R}_{12}\cdot(\vec{\mu}_1 \times \vec{\mu}_2)V_{12} \tag{1}$$

In eq 1, vectors $\vec{\mu}_1$ and $\vec{\mu}_2$ denote the direction and magnitude of the coupled transition dipole moments, and vector $\vec{R}_{12} = \vec{R}_2 - \vec{R}_1$, points from the location of transition dipole moment 1 to 2. The interaction energy, V_{12}, is often estimated using the point-dipole approximation:

$$V_{12} = \frac{\mu_1\mu_2}{R_{12}^3}[\hat{\mu}_1\cdot\hat{\mu}_2 - 3(\hat{\mu}_1\cdot\hat{R}_{12})(\hat{\mu}_2\cdot\hat{R}_{12})] \tag{2}$$

where $\hat{\mu}_1$, $\hat{\mu}_2$, and $\hat{R}_{12}$ are dimensionless unit vectors that point in the direction of $\vec{\mu}_1$, $\vec{\mu}_2$, and $\vec{R}_{12}$, respectively. By combining eqs 1 and 2, the ECCD signal strength is seen to vary inversely as the square of the distance between the coupled chromophores. Although the dipole−dipole approximation (eq 2) may fail to predict the precise coupling strength due to the short distance between the stacked bases,[64−67] eq 1 should nevertheless correctly predict the sign of the ECCD couplet.

The hallmark of degenerate exciton coupling in the CD spectrum of a multichromophoric system is the appearance of two overlapping Cotton effects of opposite sign, which are centered symmetrically about the frequency of the coupled transition. According to eq 1, ECCD vanishes whenever the two transition dipole moments lie in the same plane. Nonzero signals are therefore observed only when the coupled transition dipole moments form a chiral arrangement in space. Importantly, the sign of $\vec{R}_{12}\cdot(\vec{\mu}_1 \times \vec{\mu}_2)V_{12}$ determines the sign of the longer-wavelength Cotton effect, a result known as the exciton chirality rule of Nakanishi and Harada.[63] The bright $\pi\pi^*$ transitions of the nucleobases are in-plane transitions. When the bases lie in parallel planes (cofacial stacking), the coupled transition dipole moments, $\vec{\mu}_1$ and $\vec{\mu}_2$, are related by a screw axis. For a right-handed screw axis (positive torsion angle), the sign of $\vec{R}_{12}\cdot(\vec{\mu}_1 \times \vec{\mu}_2)V_{12}$ is positive, and a positive couplet (i.e., positive Cotton effect followed immediately by a negative one at shorter wavelength) is observed as seen for dApdA in aqueous solution (Figure 1a). On the other hand, a left-handed screw axis (negative torsion angle) produces a negative couplet like the ones seen in the CD spectra of Ap_4A and Ap_5A in aqueous solution (Figure 1b).

We next discuss how the torsion angles defined by the coupled transition dipole moments are obtained from a general specification of the geometry of two cofacially stacked bases. In addition to specifying the twist angle between the bases and any lateral displacement, it is necessary to describe how the distinguishable faces of the two bases are oriented. As already mentioned, the nucleobases have two distinguishable sides like a coin or playing card on account of their low symmetry. If the six-membered pyrimidine ring of a purine like adenine is viewed as a clock face with the C6 atom oriented toward 12 o'clock, then a viewer is looking at the side denoted α or "face" when the five-membered imidazole ring is closest to the 9 o'clock position (the α face faces the reader in the adenine structure in Chart 1). The opposite side is denoted β or "back". This nomenclature agrees with the convention of Rose et al.[68] and earlier discussions of stacking by 5′,5′-diadenosine oligophosphates.[34,35,69,70]

Bases on the same strand of a double helix usually face in the same direction such that a viewer looking down a strand from the 5′ end toward the 3′ end sees only the β sides of the purines.[68] Adjacent adenines in DNA therefore stack with the α side of the 5′ base against the β side of the 3′ base, a motif known as face-to-back stacking.[33] Dinucleosides with sufficiently flexible linkers as well as base monomers that self-associate may also form $\alpha-\alpha$ (face-to-face) and $\beta-\beta$ (back-to-back) stacks. Unfortunately, these symmetric stacking motifs are frequently referred to indiscriminately as "face-to-face" in the literature, even though they are not superposable and generally have different interaction energies.

Geometry and Axial Chirality of Cofacial Base Stacks. For simplicity, we ignore displacement of the two bases, which does not change the torsion angles between coupled dipole moments and has a secondary effect on the appearance of the CD spectrum. In this case, the geometry of a cofacial stack is fully specified by the stacking motif ($\alpha-\alpha$, $\alpha-\beta$, etc.) and the twist angle R defined as the (signed) torsion angle between vectors pointing from C4 to C5 in each purine base. We write $X_{\alpha-\beta}Y$ for a stack in which the α side of base X (top base) is stacked against the β side of base Y (bottom base). With this definition, a $\beta-\alpha$ stack with positive twist angle R is produced by starting from the $R = 0$ geometry and rotating the bottom base clockwise by R degrees. Flipping (180° rotation) either base about its C4−C5 axis produces an $\alpha-\alpha$ or $\beta-\beta$ stack without changing the value of R. Table 1 summarizes enantiomeric relationships among the various stacking motifs. Because the mirror image of an $\alpha-\alpha$ stack has $\beta-\beta$ stacking, and vice versa, $\alpha-\alpha$ and $\beta-\beta$ stacks are chiral for all values of the twist angle. Recognizing enantiomeric stacks (neglecting the backbone) is useful because such stacks have identical interaction energies, yet their ECCD spectra are mirror images of each other because their torsion angles are opposite in sign.

The preceding remarks make it possible to now discuss how the torsion angles between coupled transition dipole moments

dx.doi.org/10.1021/ja501342b | J. Am. Chem. Soc. XXXX, XXX, XXX−XXX

Table 1. Four Possible Cofacial Stacking Motifs of Two Bases X and Y

motif,[a] twist angle[b]	mirror image
$X_{\alpha-\beta}Y$, R	$Y_{\alpha-\beta}X$, $-R$
$X_{\beta-\alpha}Y$, R	$Y_{\beta-\alpha}X$, $-R$
$X_{\alpha-\alpha}Y$, R	$Y_{\beta-\beta}X$, $-R$
$X_{\beta-\beta}Y$, R	$Y_{\alpha-\alpha}X$, $-R$

[a]X and Y are the top and bottom bases, respectively. The subscript closest to X and Y denotes the side (α or β) of each that is oriented toward the second base. Note that turning over any stack does not change the structure, i.e., stack $X_{\alpha-\beta}Y$, R is identical to $Y_{\beta-\alpha}X$, R. [b]Defined as the torsion angle between vectors oriented in each base from C4 to C5.

depend on stacking motif and twist angle. According to Table 1, $\alpha-\beta$ and $\beta-\alpha$ stacks with twist angle R are identical structures when bases X and Y are the same, so there are only three independent stacking motifs for homodimers. For an $\alpha-\beta$ stack, the torsion angles between degenerately coupled dipole moments are the same for every in-plane transition, regardless of how each dipole is oriented in the molecular framework. This common torsion angle is simply the twist angle R.[64] In this case, every pair of degenerately coupled transition dipole moments yields CD couplets with the same sign. For example, the positive couplets centered at 188, 213, and 259 nm in the CD spectrum of dApdA indicate a dominant $\alpha-\beta$ stack in which the bases form a right-handed helix.

In symmetric homodimer stacks ($\alpha-\alpha$ or $\beta-\beta$), the torsion angle between a transition dipole moment in one base and the same dipole in the second base depends on both the twist angle and on the angle that each makes with a fixed direction in the molecular framework. If the orientation of the transition dipole moment is measured by the angle θ it makes with the C4−C5 axis (DeVoe and Tinoco convention,[71] see Figure 7a), then the desired torsion angles, η, are calculated as shown in eq 3:

$$\eta_{\alpha-\alpha} = R + 2\theta,\ \eta_{\beta-\beta} = R - 2\theta \tag{3}$$

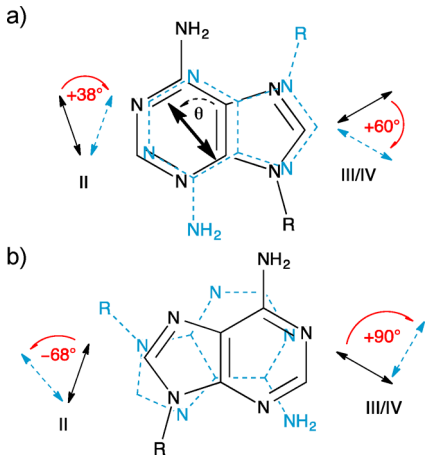

Figure 7. Proposed stacking geometries for Ap_4A and Ap_5A. The top base is shown in black, and the bottom base is shown by dashed blue lines. (a) The $\alpha-\alpha$ stack with twist angle of 180° proposed in ref 34, and (b) the $\beta-\beta$ stack with twist of 150° proposed in this study. The torsion angles between transition dipole moments for the $\pi-\pi^*$ transitions II, III, and IV (see Table 1) are shown next to each structure. Transition dipole moment directions are measured by the angle θ illustrated in (a).

Lowest $^1\pi,\pi^*$ Transitions of Adenine. Modeling ECCD spectra for $\alpha-\alpha$ and $\beta-\beta$ stacks thus requires knowledge of the transition dipole moment directions for the adenine chromophore. These directions were uncertain for many years,[72] but recent experiments and high-level calculations are now reasonably consistent for the four lowest energy $\pi \rightarrow \pi^*$ transitions of several adenine derivatives (first three rows of Table 2). These four transitions are responsible for the two broad bands seen in the absorption spectrum of adenine at wavelengths longer than 200 nm. Each band arises from an overlapping pair of $\pi \rightarrow \pi^*$ transitions. The two lowest transitions (I and II) are centered at 272 and 258 nm for 9-methyladenine in aqueous solution, but the oscillator strength of transition I is five times weaker than that of transition II.[73] Overlapping transitions at 213 nm (III) and 217 nm (IV) have comparable oscillator strength[73] and are responsible for the second, more intense absorption band of adenine.

The experimental studies in Table 2 measured polarized reflection from single crystals of 2′-deoxyadenosine[74] and linear dichroism of 9-methyladenine in a stretched polymer film.[73] The theoretical study by Marian used DFT multireference configuration interaction calculations with the TZVP+Ryd basis set to calculate transition dipole moment directions for 9H-adenine.[75] The θ values from all three studies agree reasonably well for transitions I and II. There is consistency for transition III, if the alternative value of −57° from Holmén et al.[73] is used in place of their preferred value of −21°.[75] With this substitution, the calculations by Marian and the linear dichroism measurements of Holmén et al.[73] predict that transition IV is polarized in nearly the same direction as III, which lies very close to it in energy. The estimate of +15° by Clark for IV disagrees with the other studies, but this single crystal reflectivity study is more likely to be affected by excitonic interactions among nearby chromophores than the stretched polymer film experiments of Holmén et al.,[73] in which the adenines are on average more distant from each other. For this reason, we prefer the value of −64° obtained from the latter study—a value that agrees satisfactorily with the theoretical estimate of −50°.[75] In the following, we will use the Holmén et al.[73] values from the first row of Table 1 to predict the sign of couplets in the ECCD spectra of adenine dimers for various cofacial stacking geometries.

Excimer Lifetimes Are the Same for Different Stacking Motifs. Although each diadenosine studied has a distinctive CD signature, the ECCD spectra of the 5′,5′-diadenosine oligophosphates are the most unusual with their negative long-wavelength couplets. These negative couplets indicate that the coupled transition dipole moments are related by a left-handed screw axis in contrast to the right-handed screw axis in dApdA (and in ApA[19]). However, as shown above, a left-handed torsion angle can be observed even with right-handed twist ($R > 0$) in an $\alpha-\alpha$ or $\beta-\beta$ stacking motif. Scott and Zamecnik (SZ, hereafter) first proposed that these compounds do not stack in a face-to-back motif.[34] They showed that the longest wavelength couplet in the ECCD spectra of ApA and Ap_2A is positive, but negative for Ap_3A and Ap_4A. Because the zero crossing for Ap_nA dimers with $n > 1$ occurs at longer wavelength than for ApA, SZ proposed that the weaker transition I is responsible for the long-wavelength couplets and argued that no couplet is seen for transition II because the stacking geometry positions the transition II dipole moments approximately at a right angle. In particular, SZ proposed $\alpha-\alpha$

dx.doi.org/10.1021/ja501342b | J. Am. Chem. Soc. XXXX, XXX, XXX−XXX

Table 2. Transition Dipole Moment Directions in Degrees[b] for the Four Lowest $\pi \rightarrow \pi^*$ Transitions (I–IV) of Several Adenine Derivatives[a]

	I	II	III	IV	ref
9-methyladenine	66 (0.047)	19 (0.24)	−57[c] (0.14)	−64 (~0.12)	73
2′-deoxyadenosine	67 (0.09)	35 (0.18)	−45 (0.25)	15 (0.11)	74
9H-adenine	80 (0.034)	45 (0.317)	−61 ([d])	−50 (0.526)	75
adenine	52 (~0)	147 (0.30)	124(03.7[δ])	[e]	76

[a]Oscillator strengths for each transition are shown in parentheses. [b]Measured according to the DeVoe and Tinoco convention illustrated in Figure 7a. [c]The authors of ref 73 preferred a direction of −21° for this transition s but also reported the alternative value shown here. An additional transition reported by the authors of ref 73 at 230 nm is not included because it has not been seen in other studies and because its oscillator strength (f = 0.027) is too small to contribute to the ECCD spectra. [d]Not reported. [e]Authors assumed absorption band at 207 nm is due to a single transition.

stacking for Ap_3A and Ap_4A (Figure 7a) and β–β stacking for Ap_2A with a twist angle of 180° for each.

There are several problems with these assignments. First, the stacking geometries proposed by SZ for Ap_2A and Ap_3A/Ap_4A are enantiomers, if only the bases are considered. If this were correct, then the ECCD spectra should exhibit perfect mirror symmetry at all wavelengths as seen for stacks that are true mirror images of each other such as the diadenosines made with L- vs D-ribose.[77] In fact, the CD spectra of Ap_2A and the longer oligophosphates lack mirror symmetry at wavelengths below 240 nm. The CD spectrum of Ap_2A (see Figure 1 in ref 78) and the CD spectra of Ap_4A and Ap_5A (this study, Figure 1b) all exhibit a negative peak just below 220 nm, suggesting that the stacked conformations adopted by Ap_2A and by Ap_nA with n > 2 cannot be enantiomers.

Second, SZ's assignment of the long-wavelength couplet seen in the CD spectra of the diadenosine oligophosphates to transition I is problematic given its very low oscillator strength (Table 2), which is at least five times smaller than that of transition II.[65,73] Given that ECCD is proportional to the fourth power of the transition dipole moment or, equivalently, the square of the oscillator strength (eqs 1 and 2), transition I is too weak to account for the long-wavelength CD signals from Ap_4A and Ap_5A, which are approximately one-half as intense as in dApdA (Figure 1b). The long-wavelength couplet in the ECCD spectra should therefore be reassigned to excitonic coupling among the transition II dipole moments.

Finally, as pointed out in ref 35, the SZ analysis is based on transition dipole moment directions from early Hueckel molecular orbital theory calculations.[76] These values, which are shown in the last row of Table 2, disagree significantly with today's consensus values. Using the transition dipole moment directions from Holmén et al.[73] (row 1 in Table 2) and assuming α–α stacking with a twist angle of 180° as proposed by SZ, eq 3 predicts torsion angles of −48°, +38°, and +66° for transitions I, II, and III, respectively. These angles, which predict positive couplets for the strong transitions II and III, are inconsistent with the experimental spectrum, allowing this stacked geometry to be ruled out.

Although the twist angle proposed by SZ is most likely in error, their conclusion that the diadenosine oligophosphates adopt a symmetric stacking motif is supported by experimental evidence. A decisive observation in support of their conclusion is the strong positive couplet with zero crossing at 213 nm seen for dApdA, which is replaced in Ap_4A and Ap_5A by a negative couplet of greatly reduced amplitude with a shorter wavelength zero crossing (Figure 1b). In fact, the CD spectra of Ap_4A and Ap_5A are similar to that of the monomer ATP below 230 nm. The intense UV absorption seen near 213 nm (transitions III and IV) should give even greater rotational strength than the long-wavelength couplet assigned to transition II (and both couplets should have the same sign), if the torsion angles between dipole moments were all the same, as would be the case if only α–β stacks were present. The absence of a strong 213 nm couplet in Ap_4A and Ap_5A is therefore best explained by face-to-face (or back-to-back) stacking as only these arrangements can cause cancellation of some, but not all couplets due to θ-dependent torsion angles.

Next, we consider what stacking geometry best explains the observed CD signals from the oligophosphates given the modern θ values for adenine (Table 2). An important caveat is that the stacked state of any dinucleoside or dinucleotide is unlikely to be a unique conformation.[18,38,79,80] Instead, dinucleosides are likely to populate a broad distribution of stacked conformers in aqueous solution. In this case, the ECCD spectrum can at best provide information about the average geometry of a base stack. For the diadenosine oligophosphates, the very weak CD signal seen at 213 nm for Ap_4A and Ap_5A suggests that the twist angle is such that the transition dipole moments from the strong transitions III/IV make an angle of 0° or 90°, while the transition dipole moments from transition II make a negative torsion angle consistent with the negative couplet seen for these compounds. This will be the case (assuming $\theta_{III/IV} \approx -60°$, first row of Table 2) for R = −60° or +120° for an α–α stack or for R = −30° or +150° for a β–β stack. There are two values of R in each case because rotating either base by 180° about an axis perpendicular to the base plane does not change any of the torsion angles between coupled, in-plane dipole moments.

It is difficult to choose among these possibilities, but some evidence supports assignment of α–α stacking to shorter oligophosphates and β–β to the longer ones. Thus, Thornton and Bayley found that α–α was the most common motif in lowest energy structures calculated for Ap_2A using semi-empirical methods.[69] Potential of mean force calculations by Stern et al. revealed that the free energy well for α–α stacking by Ap_2A is twice as deep as for β–β stacking (3.1 vs 1.5 kcal mol^{-1}).[35] Results were less conclusive for Ap_4A, but β–β stacking is seen in the X-ray crystal structure of Ap_4A.[81] We propose that in Ap_4A and Ap_5A stacks are predominantly β–β with a twist angle close to +150° (Figure 7b). Interestingly, a similar geometry was proposed for stacking by aggregates of adenosine[18] and 5′-AMP.[82] It is possible that the longer linkers found in Ap_4A and Ap_5A eliminate constraints imposed by shorter ones, allowing the two adenines to adopt the minimum-energy geometry found in the aggregates.

Implications for Nonradiative Decay in Oligonucleotides. Although the twist angle may be uncertain, the evidence

dx.doi.org/10.1021/ja501342b | J. Am. Chem. Soc. XXXX, XXX, XXX–XXX

discussed above strongly indicates that the two diadenosine oligophosphate compounds have symmetric ($\alpha-\alpha$ or $\beta-\beta$) stacking motifs, whereas the three DNA diadenosines form face-to-back stacks. Despite differences in the stacked geometries present at the instant of photon absorption, the excimers decay with the same lifetime within experimental uncertainty. Previously, it was shown that poly(A) and poly(dA)[6] and oligo(A) and oligo(dA)[8] have similar excimer lifetimes. Lifetimes of long-lived excited states in an alternating GC-duplex are also identical within experimental uncertainty regardless of whether the duplex is present as a B- or Z-form helix,[83] although relaxation in these systems could be influenced by base pairing.

Temps and co-workers have suggested that twisting and other motions that occur on time scales of several ps are required to move the Franck–Condon excited state to a stabilized excimer state.[52] However, the hypothesis that a common lifetime reflects a common excimer geometry attained after excitation appears in doubt because it is impossible to make a face-to-face stack have the same geometry as a face-to-back stack without flipping over one of the bases—a dynamical event that is likely to occur far slower than deactivation of the excimer state in a few hundred ps. Thus, the common dynamics seen for Ap_4A/Ap_5A, which likely form $\alpha-\alpha$ or $\beta-\beta$ stacks, and the other diadenosines, which do not, suggest that excimer decay is insensitive to the precise geometry of a cofacial stack. Furthermore, the argument has been made elsewhere that excimers are populated in <200 fs,[8] i.e., faster than twisting or other large-scale nuclear motions, which could alter the initial stacked geometry. If this is correct, then neither excimer formation nor decay appears to be sensitive to the precise stacking geometry as long as the bases are cofacially stacked.

Stacked Bases Can Fail to Give ECCD Spectra. Another conclusion from this study is that excimer states detected in a TA experiment can more reliably indicate base stacking than an ECCD spectrum. The bases in dApC3pdA and dApTHFpdA are stacked because their TA signals show the signature of excimers (Figure 4a), yet the CD spectra of these dimers lack ECCD features and resemble the CD spectrum of dAMP (Figure 1a). The absence of an ECCD spectrum for a dinucleoside or single-stranded oligonucletotide has often been interpreted to mean that all bases are unstacked. For example, Dolinnaya and Fresco[84] concluded that dApdG is unstacked because its CD spectrum at pH 4 and 3 °C is similar to that recorded at high temperature and in 80% methanol. Kang et al.[85] observed monomer-like CD spectra between 2 and 90 °C for adenine dimers joined by a neutral backbone made of carbonyl-linked 2′-deoxyribosyl groups and concluded that the bases are unstacked in these dimers. Although we have not investigated whether these systems are stacked or not, our TA results conclusively demonstrate stacked dinucleoside structures that lack ECCD signals, and caution that a CD spectrum that lacks excitonic interactions is not a foolproof indicator of unstacked conformations.

In order to not give ECCD signals, the stacked conformations adopted by dApC3pdA and dApTHFpdA could be axially achiral, as when a homodimer with $\alpha-\beta$ stacking has a twist angle of 0° or 180°, but we consider it more likely that a racemic distribution of stacked structures is present with essentially equal numbers of left- and right-handed helical conformations. The greater length of the linkers in dApC3pdA and dApTHFpdA may permit stacked conformers to adopt either helicity with equal probability. A broad distribution of conformations[86] is reasonable in light of the small free energy of stacking that is comparable in magnitude to k_BT at room temperature. This inference is supported by MD simulations, which show that single-stranded nucleic acids are highly dynamic and readily fold and unfold at room temperature.[87] The absence of deeply trapped structures is one reason why defining geometrical criteria for identifying base-stacked conformers from the broad distribution of structures that occur in a typical MD trajectory is challenging.[88,89] Furthermore, there is growing evidence that the force fields used in MD simulations overstabilize base stacking,[17] and the actual distribution of structures may be even broader and more dynamic than suggested by the simulations.

ECCD Spectra Can Arise from Unstacked Bases. Interestingly, the CD spectrum of dApdA in 80% methanol (Figure 2a) exhibits a weak, positive couplet even though the TA signal (Figure 6a) lacks a slow decay component, indicating an unstacked conformation. The constancy of UV hypochromism for dApdA in 80% methanol (Figure S5) is a further indication that the bases are unstacked. Hypochromicity decreases sharply with interbase separation and is largest when the bases are in van der Waals contact with maximal base–base overlap.[26,76,90] Earlier, Browne et al.[91] described a bis(adenine) compound joined by a trimethylene linker with negligible hypochromism in 95% ethanol, consistent with an absence of stacking. The disappearance of excimers in the TA signals and the absence of UV hypochromism indicate that the bases are no longer in van der Waals contact in 80% methanol. The residual ECCD spectrum nonetheless indicates that the distribution of extended conformations retains a measure of axial chirality.

The preference for right-handed helicity in unstacked dApdA in 80% methanol may be a consequence of its short phosphodiester linker. Notably, none of the diadenosines with longer linkers exhibit residual ECCD signals in methanol. The phosphodiester linker also produces residual helicity in unstacked structures formed in poly(A) in 98% ethanol at 0 °C[19] and in dApdA at low pH (Figure 3). The attenuated positive couplet seen in 80% methanol vs aqueous solution (Figure 3) may be partly due to the greater distance between the nucleobases (increasing distance between the bases without changing orientation will reduce CD without changing its shape[92]), but this is unlikely to be a primary factor in the disappearance of ECCD. After all, exciton coupling is a relatively long-range interaction ($1/r^2$, see eqs 1 and 2), and ECCD signals are easily seen in bis(porphyrins) in which the chromophores are separated by 23 Å[93] and between stilbenes separated by 11 AT base pairs (~40 Å) in DNA conjugates.[94] Instead, the short phosphodiester linker likely produces a broader distribution of helical and nonhelical conformations.

■ CONCLUSIONS

Five dinucleosides with different backbones were studied by time-resolved and steady-state electronic spectroscopy in order to understand how conformation affects excited states formed in single-stranded nucleic acids by UV radiation. Excited-state dynamics were investigated in aqueous solution and, for the first time, in the presence of a denaturant (methanol). In aqueous solution, the excited-state dynamics of the dimers differ strikingly from the dynamics of a single adenine monomer, while in 80% methanol the response of the dimer is monomer-like. In 80% methanol, all of the diadenosines are unstacked, and intervening solvent molecules separate the

dx.doi.org/10.1021/ja501342b | J. Am. Chem. Soc. XXXX, XXX, XXX–XXX

bases, confirming the primary role of hydrophobic interactions in stabilizing stacked bases. Interestingly, MD simulations of ApA predict that the two adenine units are stacked most of the time in neat methanol.[95] Our conclusion that all five dinucleosides are fully unstacked in 80% methanol thus provides supporting evidence that the empirical force fields used in MD simulations overstabilize base stacking.[17,96]

All diadenosines studied have significant populations of stacked conformations in aqueous solution, even though ECCD spectra indicate that the distribution of twist angles and stacking motifs (face-to-back, face-to-face, etc.) differ depending on the linker joining the bases. Two diadenosines surrounding abasic site mimics (dApTHFpdA and dApC3pdA) can stack but lack ECCD signals, suggesting that the distribution of stacked conformers is racemic with equal numbers of left- and right-handed conformers. These observations clearly demonstrate that the nature of the backbone, and not just intrinsic interactions arising from base−base overlap, direct stacking conformation and helicity in nucleic acids.

Although excimers seen in TA signals reliably diagnose base stacking, the excimer lifetimes are insensitive to the stacking motif and twist angle. The short-range character of the interaction that leads to excimer state formation ensures that the TA signals arise from conformers that position the bases in van der Waals contact. Nevertheless, the probability of forming an excimer state depends weakly, if at all, on twist angle and on what sides of the planar bases face each other. TA measurements are thus complementary to CD and may provide a new tool for evaluating the relative importance of the hydrophobic, electrostatic, and dispersive interactions that govern base stacking in aqueous solution. Finally, the high time resolution of the TA technique could provide new opportunities for studying the dynamics of base stacking, and comparison with MD simulations could in turn provide an avenue for improving force fields, which currently overstabilize base stacking.

■ ASSOCIATED CONTENT

Supporting Information

Full experimental details, UV absorption spectra of all compounds with supplementary discussion, TA signals of dAMP and ATP in buffer solution, short-time TA signals, UV melting curve of dApdA in 80% methanol, and tables of best-fit parameters. This material is available free of charge via the Internet at http://pubs.acs.org.

■ AUTHOR INFORMATION

Corresponding Author

kohler@chemistry.montana.edu

Notes

The authors declare no competing financial interest.

■ ACKNOWLEDGMENTS

This work was made possible by funding from the National Science Foundation (CHE-1112560) and NASA (NNX12AG77G). Stimulating conversations with Prof. Patrik Callis are gratefully acknowledged.

■ REFERENCES

(1) Crespo-Hernández, C. E.; Cohen, B.; Hare, P. M.; Kohler, B. *Chem. Rev.* **2004**, *104*, 1977.
(2) Markovitsi, D.; Gustavsson, T.; Talbot, F. *Photochem. Photobiol. Sci.* **2007**, *6*, 717.
(3) Middleton, C. T.; de La Harpe, K.; Su, C.; Law, Y. K.; Crespo-Hernández, C. E.; Kohler, B. *Annu. Rev. Phys. Chem.* **2009**, *60*, 217.
(4) Kohler, B. *J. Phys. Chem. Lett.* **2010**, *1*, 2047.
(5) Kleinermanns, K.; Nachtigallova, D.; de Vries, M. S. *Int. Rev. Phys. Chem.* **2013**, *32*, 308.
(6) Crespo-Hernández, C. E.; Kohler, B. *J. Phys. Chem. B* **2004**, *108*, 11182.
(7) Takaya, T.; Su, C.; de La Harpe, K.; Crespo-Hernández, C. E.; Kohler, B. *Proc. Natl. Acad. Sci. U.S.A.* **2008**, *105*, 10285.
(8) Su, C.; Middleton, C. T.; Kohler, B. *J. Phys. Chem. B* **2012**, *116*, 10266.
(9) Chen, H.; Meisburger, S. P.; Pabit, S. A.; Sutton, J. L.; Webb, W. W.; Pollack, L. *Proc. Natl. Acad. Sci. U.S.A.* **2012**, *109*, 799.
(10) Kozlov, A. G.; Lohman, T. M. *Biochemistry* **1999**, *38*, 7388.
(11) Eggington, J. M.; Kozlov, A. G.; Cox, M. M.; Lohman, T. M. *Biochemistry* **2006**, *45*, 14490.
(12) Vesnaver, G.; Breslauer, K. J. *Proc. Natl. Acad. Sci. U.S.A.* **1991**, *88*, 3569.
(13) Bailey, S. M.; Murnane, J. P. *Nucleic Acids Res.* **2006**, *34*, 2408.
(14) Becker, M. M.; Wang, Z. *J. Mol. Bio.* **1989**, *210*, 429.
(15) Douki, T. *J. Photochem. Photobiol., B* **2006**, *82*, 45.
(16) Schreier, W. J.; Schrader, T. E.; Koller, F. O.; Gilch, P.; Crespo-Hernández, C. E.; Swaminathan, V. N.; Carell, T.; Zinth, W.; Kohler, B. *Science* **2007**, *315*, 625.
(17) Chen, A. A.; García, A. E. *Proc. Natl. Acad. Sci. U.S.A.* **2013**, *110*, 16820.
(18) Broom, A. D.; Schweizer, M. P.; Ts'o, P. O. P. *J. Am. Chem. Soc.* **1967**, *89*, 3612.
(19) Brahms, J.; Michelson, A. M.; van Holde, K. E. *J. Mol. Biol.* **1966**, *15*, 467.
(20) Brahms, J.; Maurizot, J. C.; Michelson, A. M. *J. Mol. Biol.* **1967**, *25*, 481.
(21) Adler, A. J.; Grossman, L.; Fasman, G. D. *Biochemistry* **1969**, *8*, 3846.
(22) Tazawa, S.; Tazawa, I.; Tso, P. O. P.; Alderfer, J. L. *Biochemistry* **1972**, *11*, 3544.
(23) Olsthoorn, C. S. M.; Bostelaar, L. J.; De Rooij, J. F. M.; Van Boom, J. H.; Altona, C. *Eur. J. Biochem.* **1981**, *115*, 309.
(24) Leng, M.; Felsenfeld, G. *J. Mol. Biol.* **1966**, *15*, 455.
(25) Leonard, N. J.; Ito, K. *J. Am. Chem. Soc.* **1973**, *95*, 4010.
(26) Seyama, F.; Akahori, K.; Sakata, Y.; Misumi, S.; Aida, M.; Nagata, C. *J. Am. Chem. Soc.* **1988**, *110*, 2192.
(27) Epand, R. M.; Scheraga, H. A. *J. Am. Chem. Soc.* **1967**, *89*, 3888.
(28) Breslauer, K. J.; Sturtevant, J. M. *Biophys. Chem.* **1977**, *7*, 205.
(29) Ramprakash, J.; Lang, B.; Schwarz, F. P. *Biopolymers* **2008**, *89*, 969.
(30) Ke, C.; Humeniuk, M.; S-Gracz, H.; Marszalek, P. E. *Phys. Rev. Lett.* **2007**, *99*, 018302.
(31) Mishra, G.; Giri, D.; Kumar, S. *Phys. Rev. E* **2009**, *79*.
(32) Guckian, K. M.; Schweitzer, B. A.; Ren, R. X. F.; Sheils, C. J.; Tahmassebi, D. C.; Kool, E. T. *J. Am. Chem. Soc.* **2000**, *122*, 2213.
(33) Florián, J.; Šponer, J.; Warshel, A. *J. Phys. Chem. B* **1999**, *103*, 884.
(34) Scott, J. F.; Zamecnik, P. C. *Proc. Natl. Acad. Sci. U.S.A.* **1969**, *64*, 1308.
(35) Stern, N.; Major, D. T.; Gottlieb, H. E.; Weizman, D.; Fischer, B. *Org. Biomol. Chem.* **2010**, *8*, 4637.
(36) Cantor, C. R.; Warshaw, M. M.; Shapiro, H. *Biopolymers* **1970**, *9*, 1059.
(37) Warshaw, M. M.; Cantor, C. R. *Biopolymers* **1970**, *9*, 1079.
(38) Fornasiero, D.; Kurucsev, T. *Eur. J. Biochem.* **1984**, *143*, 1.
(39) Tinoco, I. *J. Am. Chem. Soc.* **1964**, *86*, 297.
(40) Sprecher, C. A.; Johnson, W. C. *Biopolymers* **1977**, *16*, 2243.
(41) Heyn, M. P.; Bretz, R. *Biophys. Chem.* **1975**, *3*, 35.
(42) Holler, E.; Holmquist, B.; Vallee, B. L.; Taneja, K.; Zamecnik, P. *Biochemistry* **1983**, *22*, 4924.

(43) Crespo-Hernández, C. E.; Cohen, B.; Kohler, B. *Nature* **2005**, *436*, 1141.
(44) Zhang, Y.; Chen, J.; Kohler, B. *J. Phys. Chem. A* **2013**, *117*, 6771.
(45) Middleton, C. T.; Cohen, B.; Kohler, B. *J. Phys. Chem. A* **2007**, *111*, 10460.
(46) Olaso-González, G.; Merchán, M.; Serrano-Andrés, L. *J. Am. Chem. Soc.* **2009**, *131*, 4368.
(47) Smith, V. R.; Samoylova, E.; Ritze, H. H.; Radloff, W.; Schultz, T. *Phys. Chem. Chem. Phys.* **2010**, *12*, 9632.
(48) Improta, R.; Barone, V. *Angew. Chem., Int. Ed.* **2011**, *50*, 12016.
(49) Vayá, I.; Brazard, J.; Gustavsson, T.; Markovitsi, D. *Photochem. Photobiol. Sci.* **2012**, *11*, 1767.
(50) Plasser, F.; Lischka, H. *Photochem. Photobiol. Sci.* **2013**, *12*, 1440.
(51) Spata, V. A.; Matsika, S. *J. Phys. Chem. A* **2013**, *117*, 8718.
(52) Stuhldreier, M. C.; Temps, F. *Faraday Discuss.* **2013**, *163*, 173.
(53) Banyasz, A.; Gustavsson, T.; Onidas, D.; Changenet-Barret, P.; Markovitsi, D.; Improta, R. *Chem.—Eur. J.* **2013**, *19*, 3762.
(54) Herskovits, T.; Singer, S. J. *Arch. Biochem. Biophys.* **1961**, *94*, 99.
(55) Herskovits, T. T. *Arch. Biochem. Biophys.* **1962**, *97*, 474.
(56) Powell, J. T.; Richards, E. G.; Gratzer, W. B. *Biopolymers* **1972**, *11*, 235.
(57) Cantor, C. R.; Fairclough, R. H.; Newmark, R. A. *Biochemistry* **1969**, *8*, 3610.
(58) Wilson, J. N.; Cho, Y. J.; Tan, S.; Cuppoletti, A.; Kool, E. T. *ChemBioChem.* **2008**, *9*, 279.
(59) O'Neill, M. A.; Dohno, C.; Barton, J. K. *J. Am. Chem. Soc.* **2004**, *126*, 1316.
(60) Hardman, S. J. O.; Thompson, K. C. *Biochemistry* **2006**, *45*, 9145.
(61) Neely, R. K.; Jones, A. C. *J. Am. Chem. Soc.* **2006**, *128*, 15952.
(62) Tinoco, I. *Radiat. Res.* **1963**, *20*, 133.
(63) Harada, N.; Chen, S. L.; Nakanishi, K. *J. Am. Chem. Soc.* **1975**, *97*, 5345.
(64) Bush, C. A.; Tinoco, I. *J. Mol. Biol.* **1967**, *23*, 601.
(65) Bouvier, B.; Gustavsson, T.; Markovitsi, D.; Millié, P. *Chem. Phys.* **2002**, *275*, 75.
(66) Kozak, C. R.; Kistler, K. A.; Lu, Z.; Matsika, S. *J. Phys. Chem. B* **2010**, *114*, 1674.
(67) Parker, T. M.; Hohenstein, E. G.; Parrish, R. M.; Hud, N. V.; Sherrill, C. D. *J. Am. Chem. Soc.* **2013**, *135*, 1306.
(68) Rose, I. A.; Hanson, K. R.; Wilkinson, K. D.; Wimmer, M. J. *Proc. Natl. Acad. Sci. U.S.A.* **1980**, *77*, 2439.
(69) Thornton, J. M.; Bayley, P. M. *Biopolymers* **1976**, *15*, 955.
(70) Westkaemper, R. B. *Biochem. Biophys. Res. Commun.* **1987**, *144*, 922.
(71) DeVoe, H.; Tinoco, I., Jr. *J. Mol. Biol.* **1962**, *4*, 500.
(72) Callis, P. R. *Annu. Rev. Phys. Chem.* **1983**, *34*, 329.
(73) Holmén, A.; Broo, A.; Albinsson, B.; Nordén, B. *J. Am. Chem. Soc.* **1997**, *119*, 12240.
(74) Clark, L. B. *J. Phys. Chem.* **1995**, *99*, 4466.
(75) Marian, C. M. *J. Chem. Phys.* **2005**, *122*, 104314.
(76) DeVoe, H. *J. Mol. Biol.* **1962**, *4*, 518.
(77) Tazawa, I.; Tazawa, S.; Stempel, L. M.; Ts'o, P. O. P. *Biochemistry* **1970**, *9*, 3499.
(78) Ikehara, M.; Yoshida, K.; Uesugi, S. *Biochemistry* **1972**, *11*, 836.
(79) Davis, R. C.; Tinoco, I., Jr. *Biopolymers* **1968**, *6*, 223.
(80) Lowe, M. J.; Schellman, J. A. *J. Mol. Biol.* **1972**, *65*, 91.
(81) Watanabe, D.; Ishikawa, M.; Yamasaki, M.; Ozaki, M.; Katayama, T.; Nakajima, H. *Acta Crystallogr., Sect. C: Cryst. Struct. Commun.* **1996**, *52*, 338.
(82) Schweizer, M. P.; Broom, A. D.; Ts'o, P. O. P.; Hollis, D. P. *J. Am. Chem. Soc.* **1968**, *90*, 1042.
(83) de La Harpe, K.; Crespo-Hernández, C. E.; Kohler, B. *ChemPhysChem* **2009**, *10*, 1421.
(84) Dolinnaya, N. G.; Fresco, J. R. *Proc. Natl. Acad. Sci. U.S.A.* **1992**, *89*, 9242.
(85) Kang, H.; Chou, P. J.; Johnson, W. C., Jr.; Weller, D.; Huang, S. B.; Summerton, J. E. *Biopolymers* **1992**, *32*, 1351.
(86) Lee, C.-H.; Charney, E.; Tinoco, I., Jr. *Biochemistry* **1979**, *18*, 5636.
(87) Norberg, J.; Nilsson, L. *Biophys. J.* **1995**, *69*, 2277.
(88) Norberg, J.; Nilsson, L. *J. Am. Chem. Soc.* **1995**, *117*, 10832.
(89) Jafilan, S.; Klein, L.; Hyun, C.; Florián, J. *J. Phys. Chem. B* **2012**, *116*, 3613.
(90) Kondo, N. S.; Holmes, H. M.; Stempel, L. M.; Ts'o, P. O. P. *Biochemistry* **1970**, *9*, 3479.
(91) Browne, D. T.; Eisinger, J.; Leonard, N. J. *J. Am. Chem. Soc.* **1968**, *90*, 7302.
(92) Johnson, W. C., Jr.; Itzkowitz, M. S.; Tinoco, I., Jr. *Biopolymers* **1972**, *11*, 225.
(93) Oancea, S.; Formaggio, F.; Campestrini, S.; Broxterman, Q. B.; Kaptein, B.; Toniolo, C. *Biopolymers* **2003**, *72*, 105.
(94) Lewis, F. D.; Zhang, L. G.; Liu, X. Y.; Zuo, X. B.; Tiede, D. M.; Long, H.; Schatz, G. C. *J. Am. Chem. Soc.* **2005**, *127*, 14445.
(95) Norberg, J.; Nilsson, L. *Biophys. J.* **1998**, *74*, 394.
(96) Banáš, P.; Mládek, A.; Otyepka, M.; Zgarbová, M.; Jurečka, P.; Svozil, D.; Lankaš, F.; Šponer, J. *J. Chem. Theory Comput.* **2012**, *8*, 2448.